The STIX Image Reconstruction Concept

P. Massa, F. Benvenuto, A. M. Massone and M. Piana

7th Metis Workshop, November 12, 2019

MIDA group - Methods for Image and Data Analysis
Department of Mathematics, University of Genoa

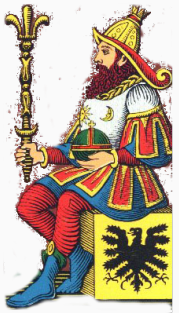

Table of contents

The STIX instrument

The instrument

STIX (Spectrometer/Telescope for Imaging X-rays) is the X-ray imager on board Solar Orbiter

The instrument

STIX (Spectrometer/Telescope for Imaging X-rays) is the X-ray imager on board Solar Orbiter

Goal

Determining the timing, location, and spectrum of accelerated electrons in the corona and chromosphere.

The instrument

STIX (Spectrometer/Telescope for Imaging X-rays) is the X-ray imager on board Solar Orbiter

Goal

Determining the timing, location, and spectrum of accelerated electrons in the corona and chromosphere.

How?

By measuring the timing, location, and spectrum of the thermal and non-thermal hard X-ray emissions.

The instrument

STIX (Spectrometer/Telescope for Imaging X-rays) is the X-ray imager on board Solar Orbiter

Goal

Determining the timing, location, and spectrum of accelerated electrons in the corona and chromosphere.

How?

By measuring the timing, location, and spectrum of the thermal and non-thermal hard X-ray emissions.

MIDA@UNIGE is involved in the ground based image and data analysis

The instrument

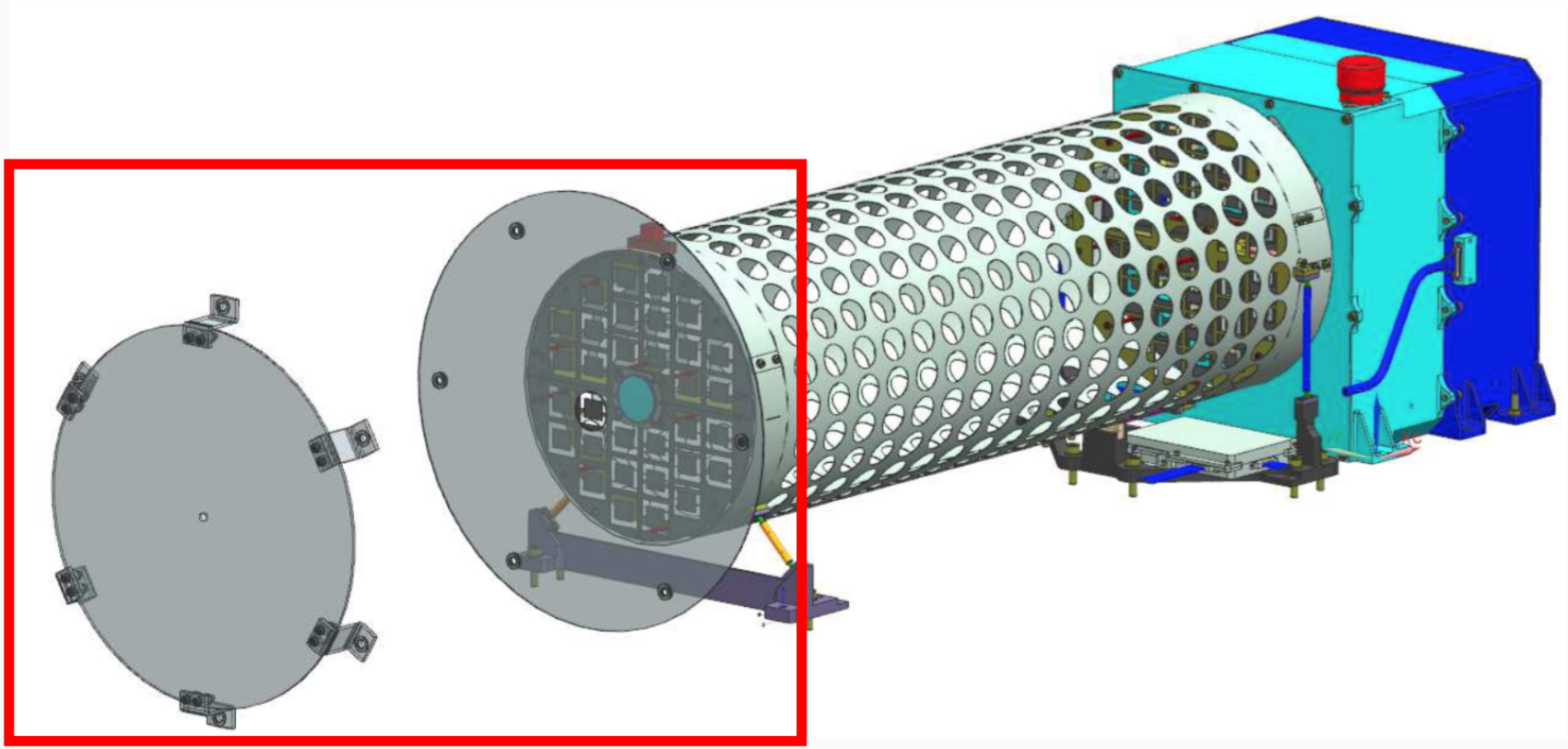

X-ray window

Benz, A.O., Krucker, S., Hurford, G.J., et al. 2012

The instrument

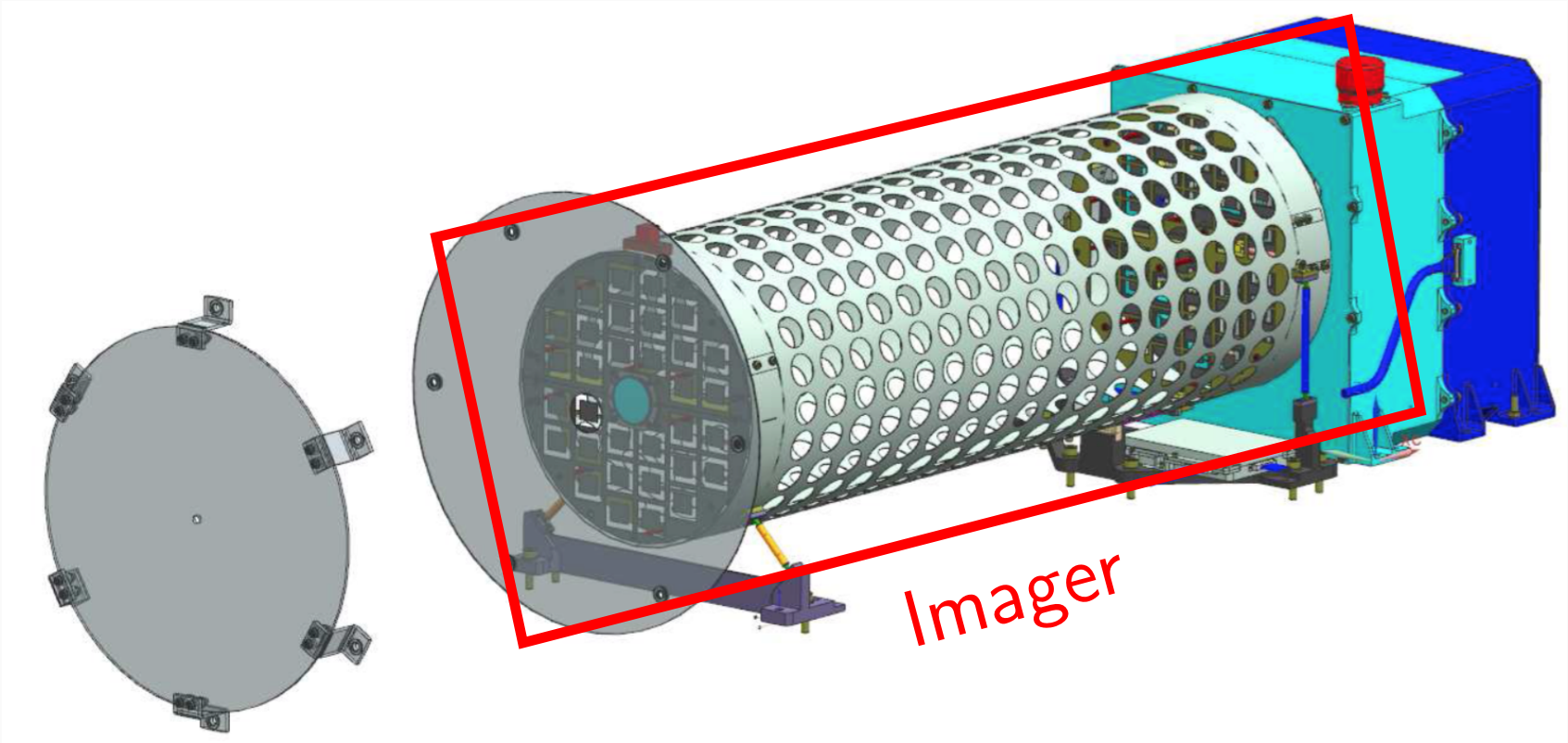

Benz, A.O., Krucker, S., Hurford, G.J., et al. 2012

The instrument

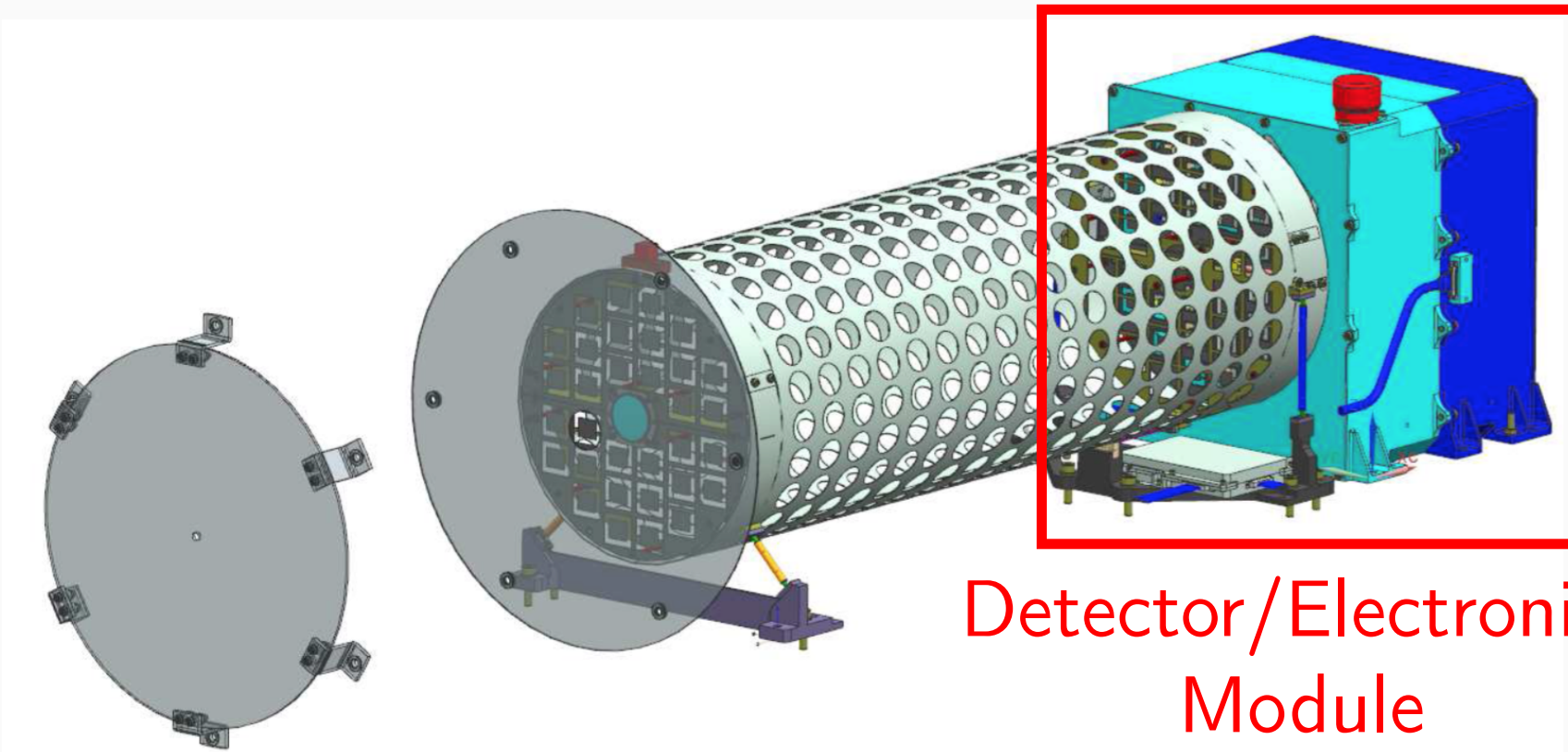

Benz, A.O., Krucker, S., Hurford, G.J., et al. 2012

X-ray window

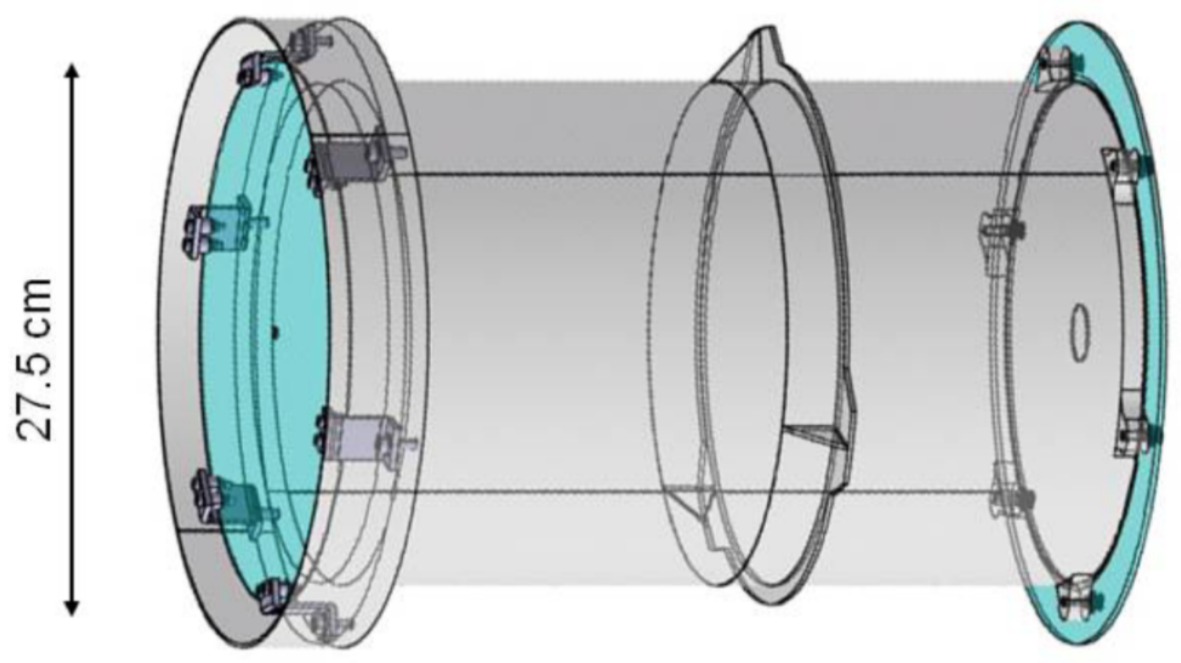

Benz, A.O., Krucker, S., Hurford, G.J., et al. 2012

Imager

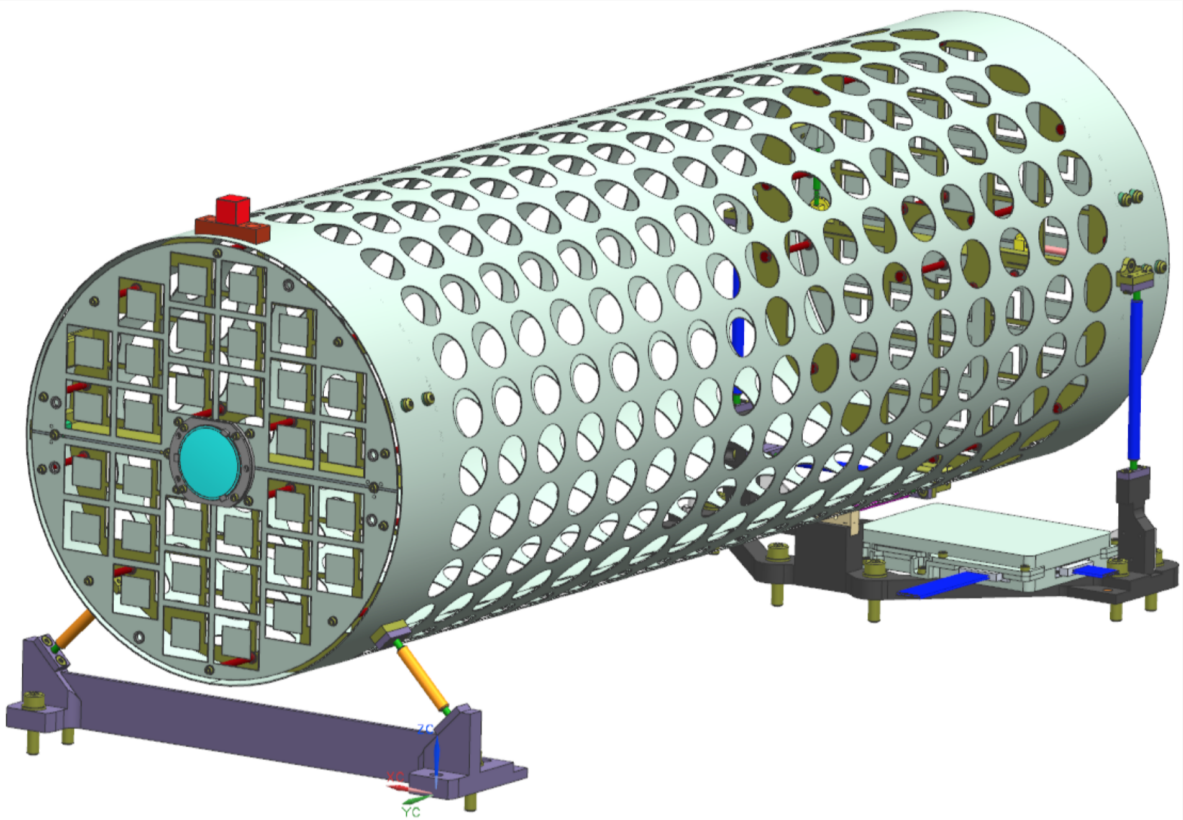

Benz, A.O., Krucker, S., Hurford, G.J., et al. 2012

Grids and Moiré pattern

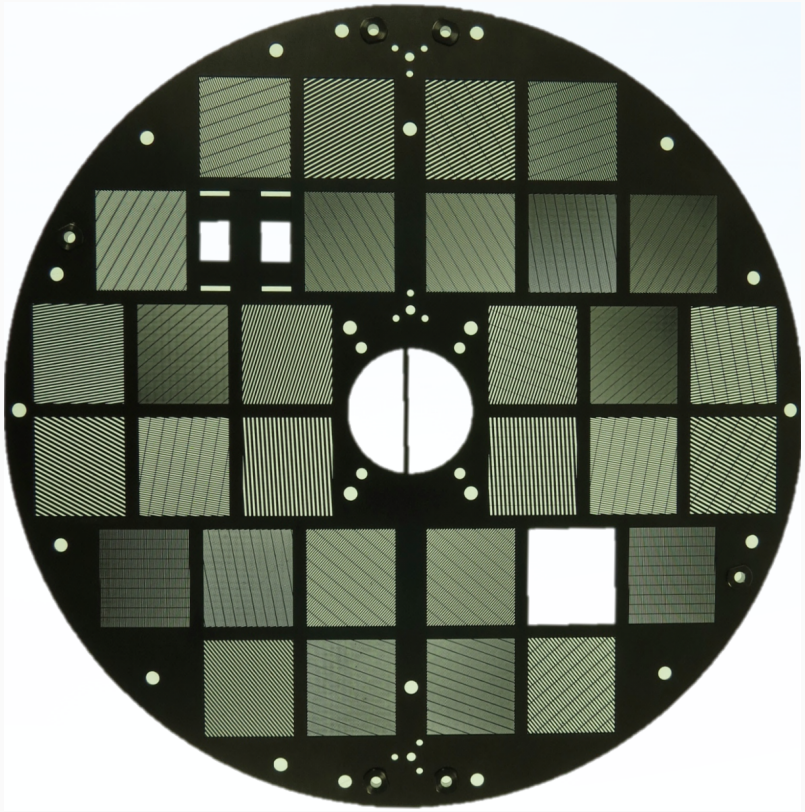

Vilmer, N., Krucker, S. et al., 2014

Grids and Moiré pattern

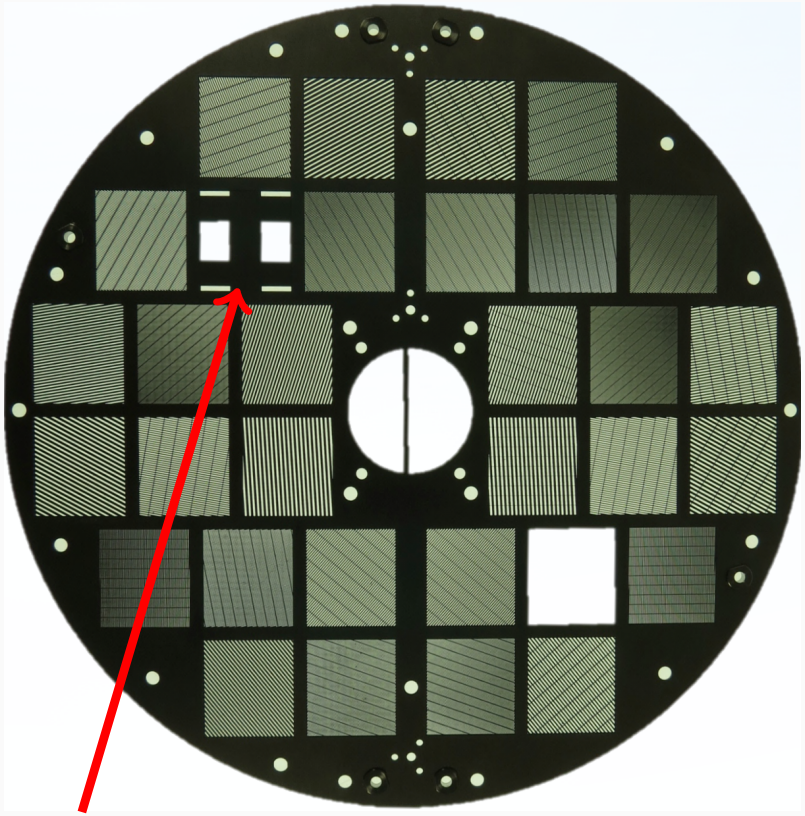

Flare locator

Vilmer, N., Krucker, S. et al., 2014

Grids and Moiré pattern

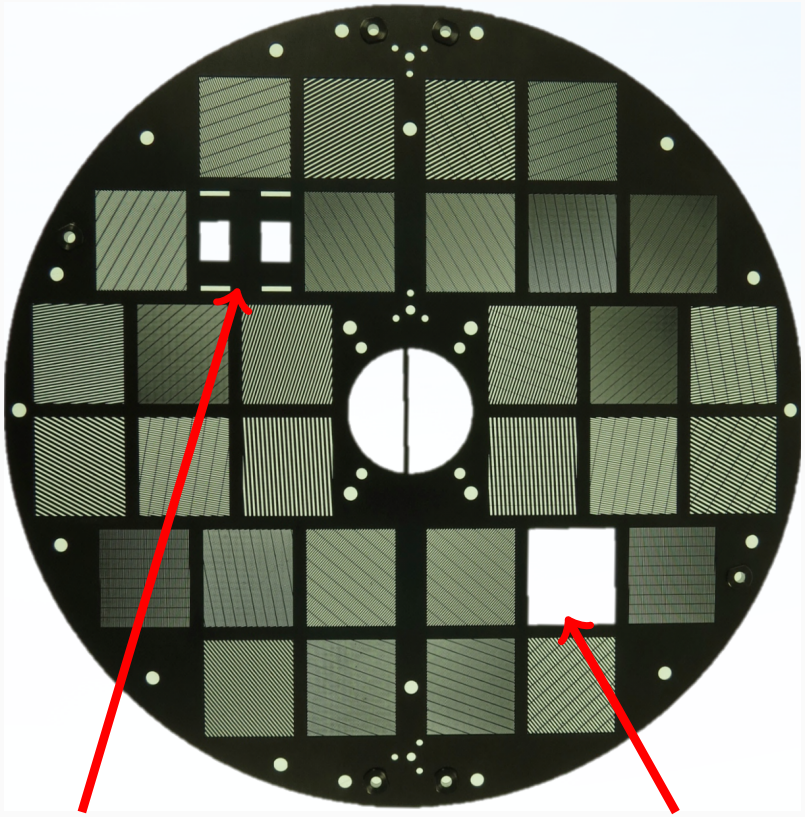

Vilmer, N., Krucker, S. et al., 2014

Grids and Moiré pattern

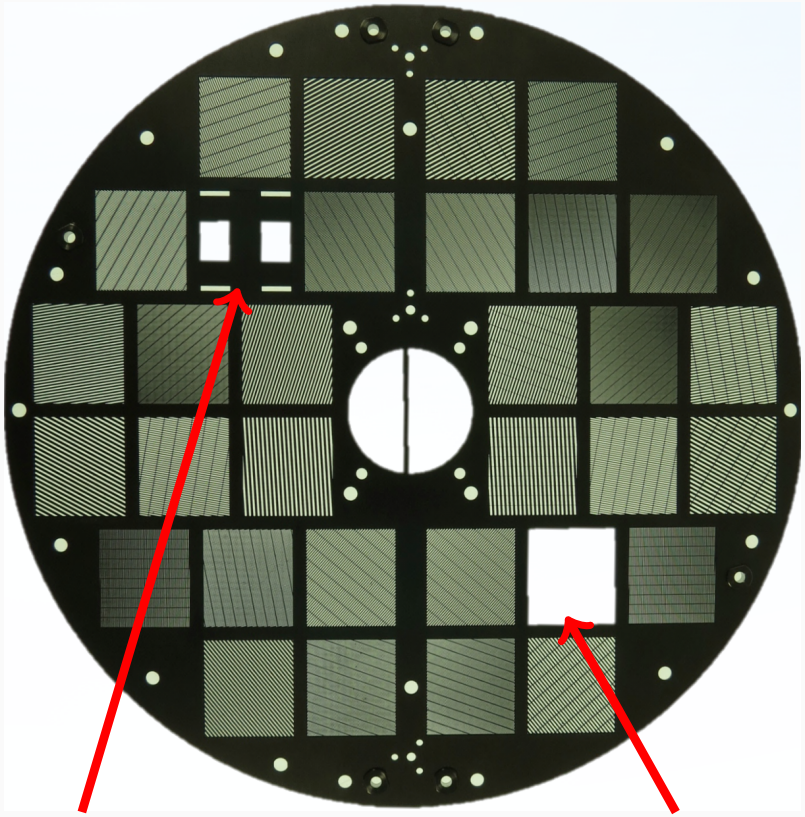

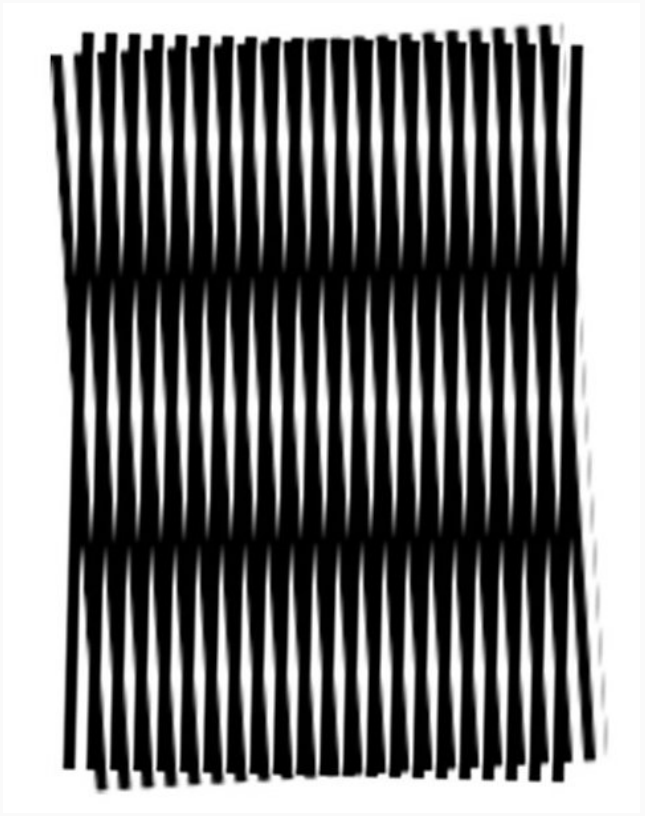

Vilmer, N., Krucker, S. et al., 2014

Detector/Electronics Module

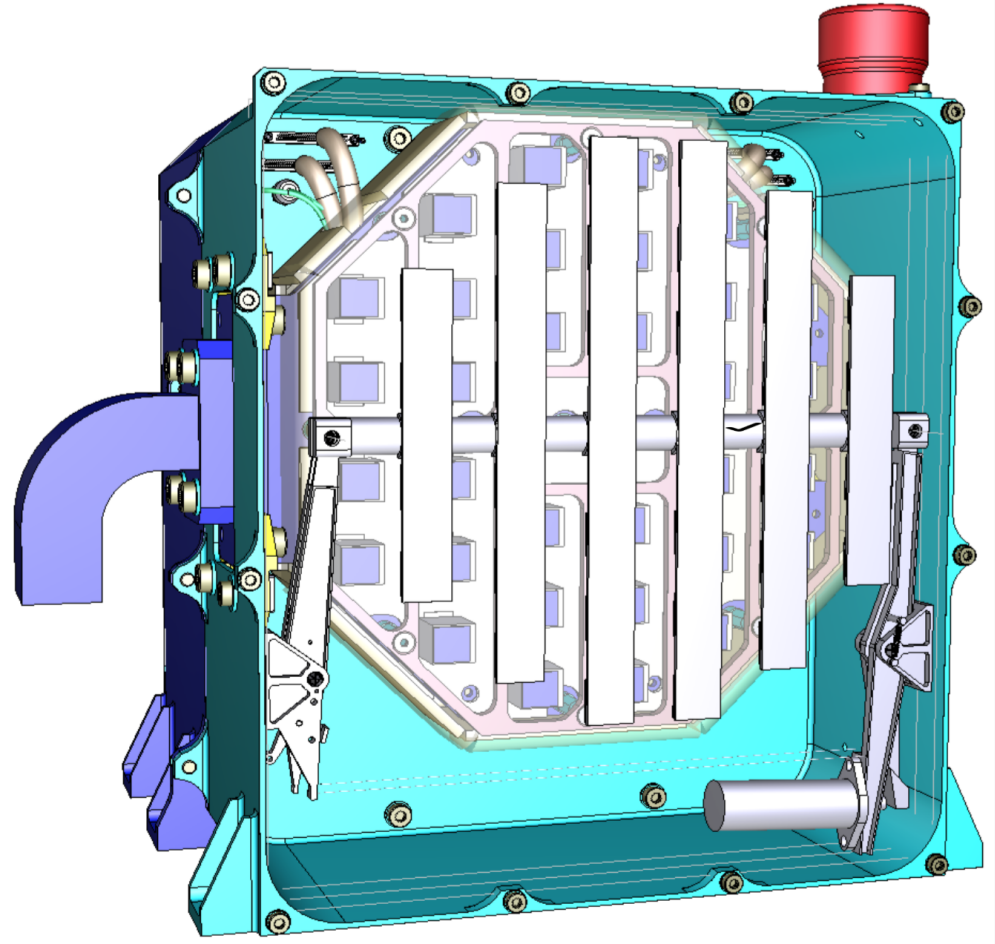

Benz, A.O., Krucker, S., Hurford, G.J., et al. 2012

Detector/Electronics Module

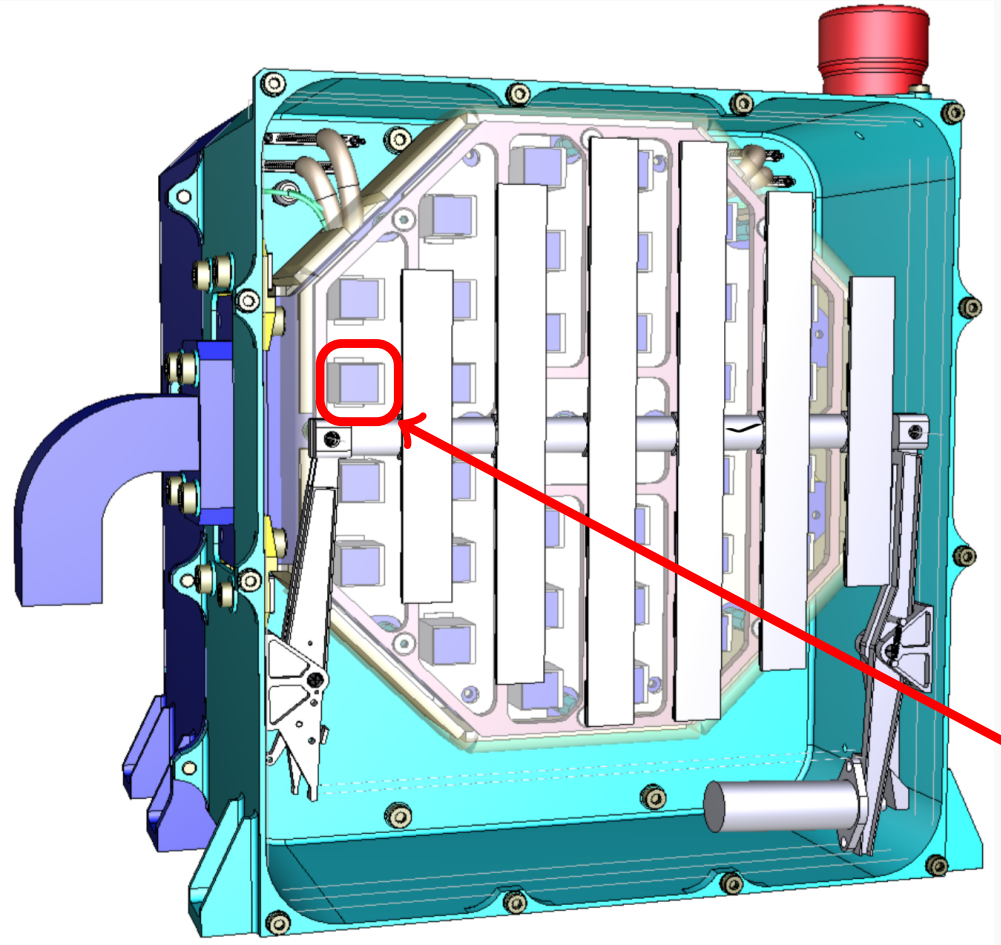

Benz, A.O., Krucker, S., Hurford, G.J., et al. 2012

Detectors

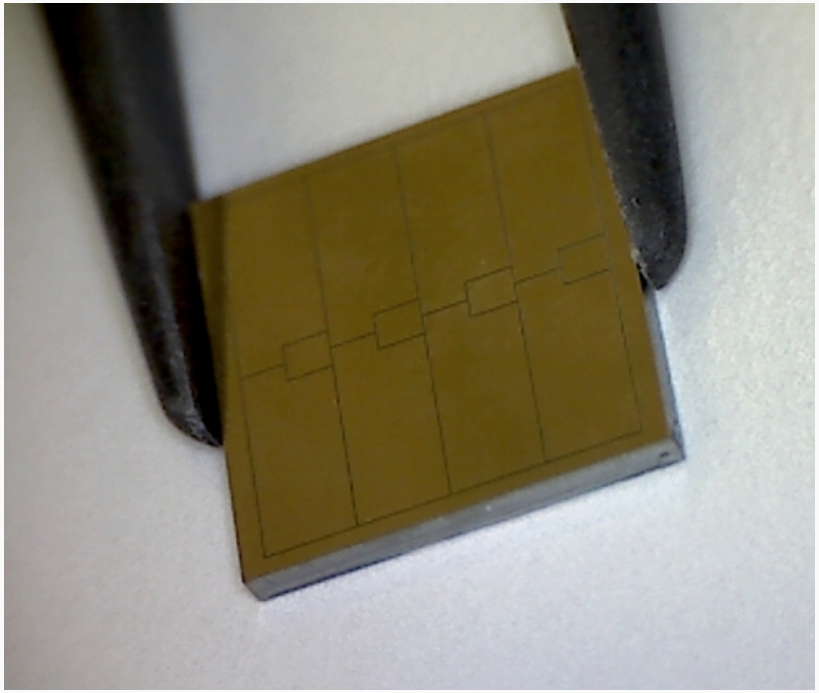

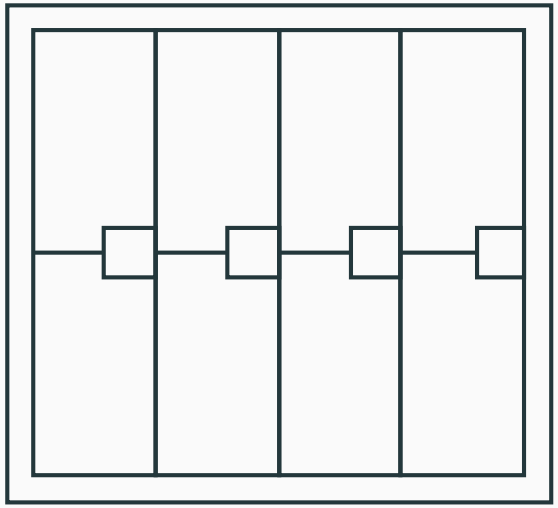

Benz, A.O., Krucker, S., Hurford, G.J., et al. 2012

Detectors

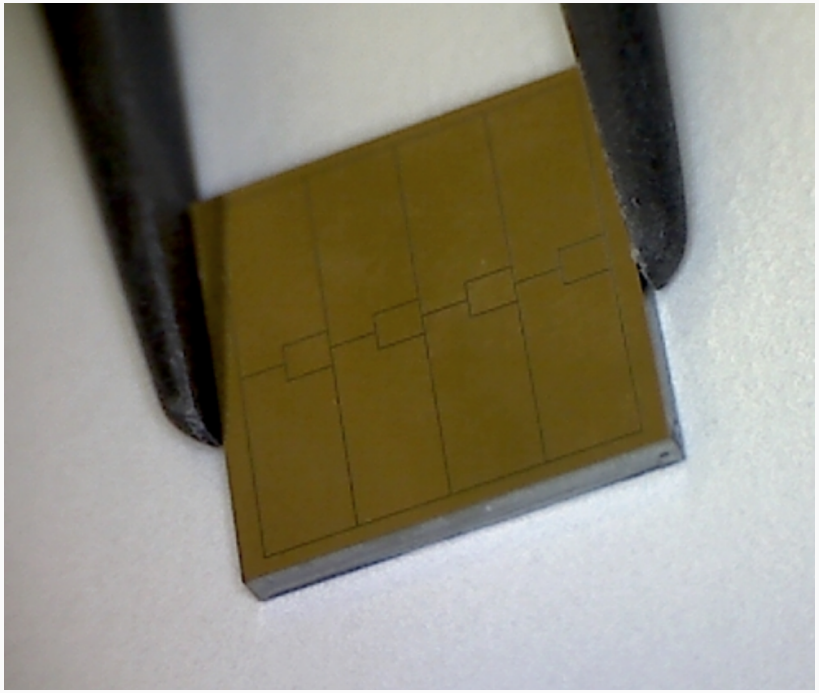

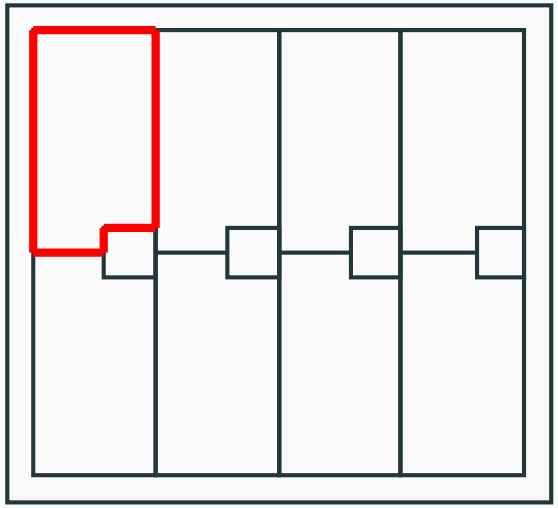

Benz, A.O., Krucker, S., Hurford, G.J., et al. 2012

Detectors

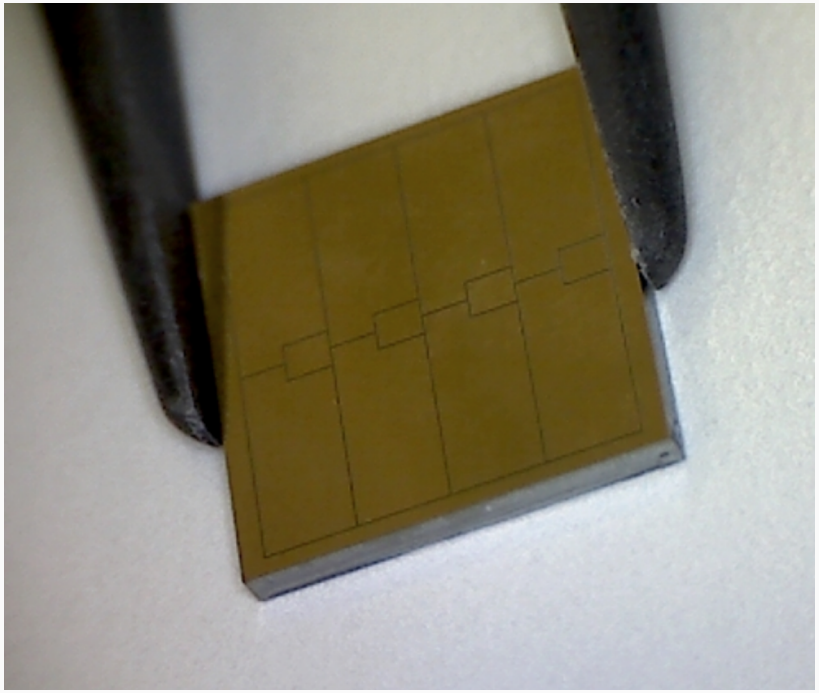

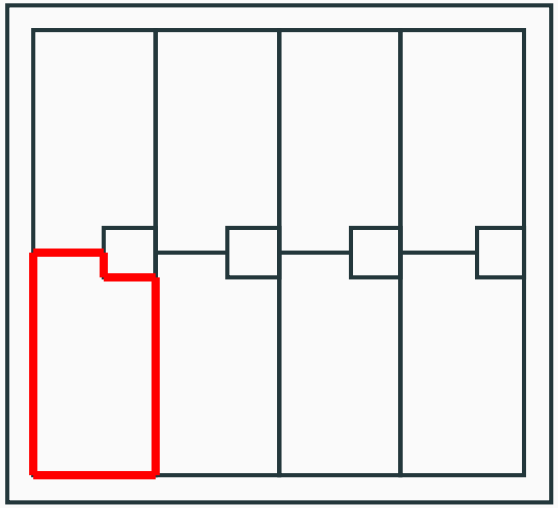

Benz, A.O., Krucker, S., Hurford, G.J., et al. 2012

Detectors

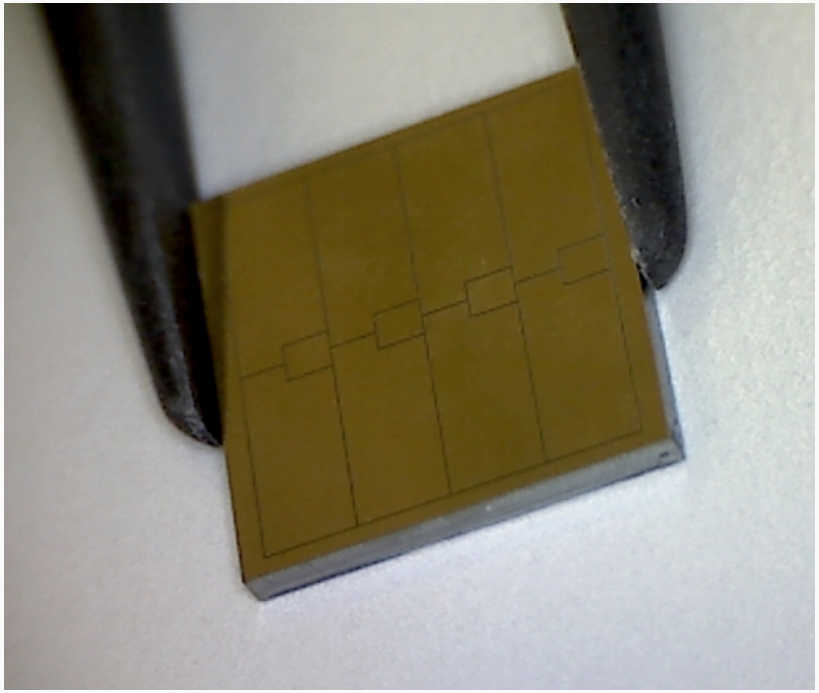

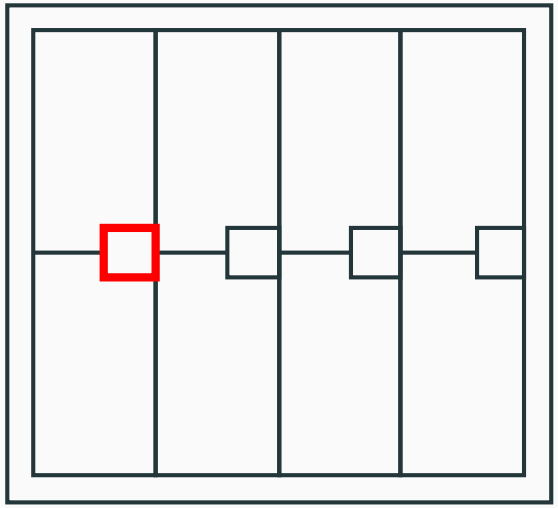

Benz, A.O., Krucker, S., Hurford, G.J., et al. 2012

Performance (Benz, A.O., Krucker, S., Hurford, G.J., et al. 2012)

- Energy range: 4-150 keV
- Energy resolution: 1-15 keV
- Finest angular resolution: 7 arcsec
- Field of view: 2°
- Image placement accuracy: $\sim$ 4 arcsec

Visibility-based imaging

Visibilities

We denote by ϕ the photon flux.

Definition

The value of the Fourier transform of ϕ

$$V(\boldsymbol{\xi}) = \int_{\mathbb{R}^2} \phi(\mathbf{x}) \exp(2\pi i \boldsymbol{\xi} \cdot \mathbf{x})\, d\mathbf{x}.$$

is named **visibility** associated to ϕ and computed at the point $\boldsymbol{\xi}$.

Fourier imaging

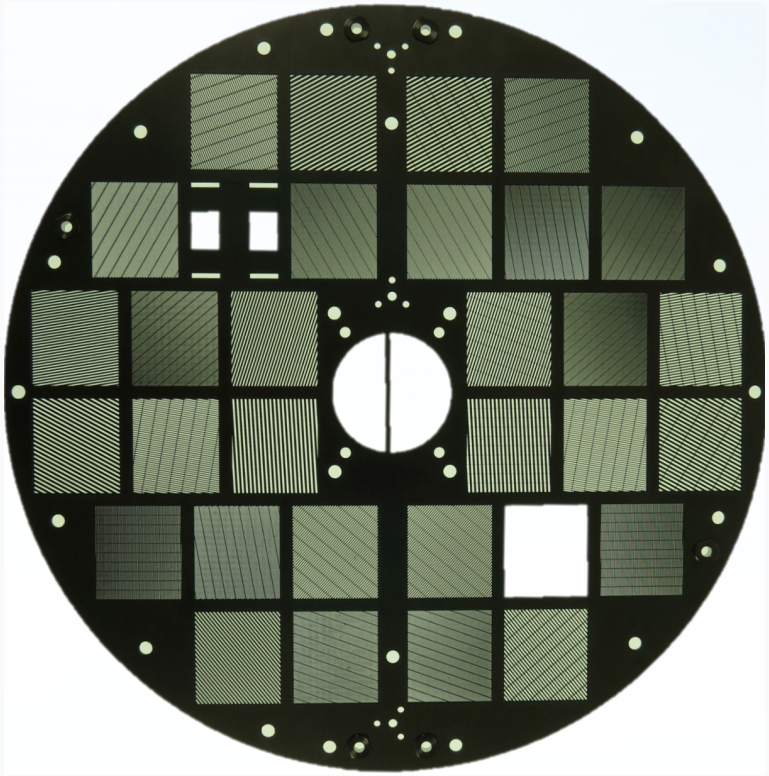

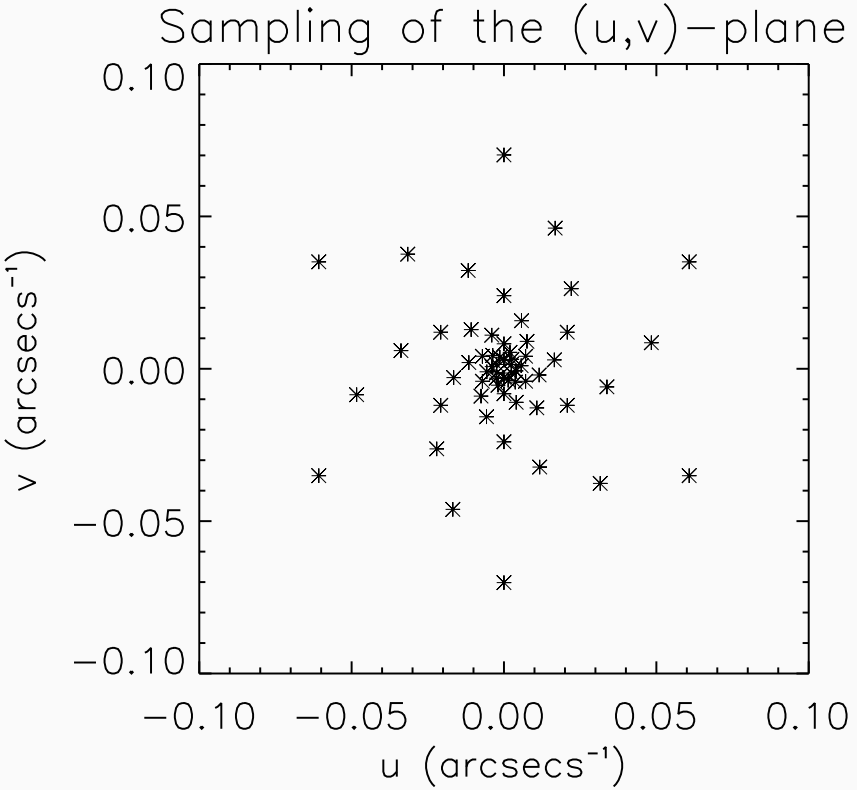

Fourier imaging

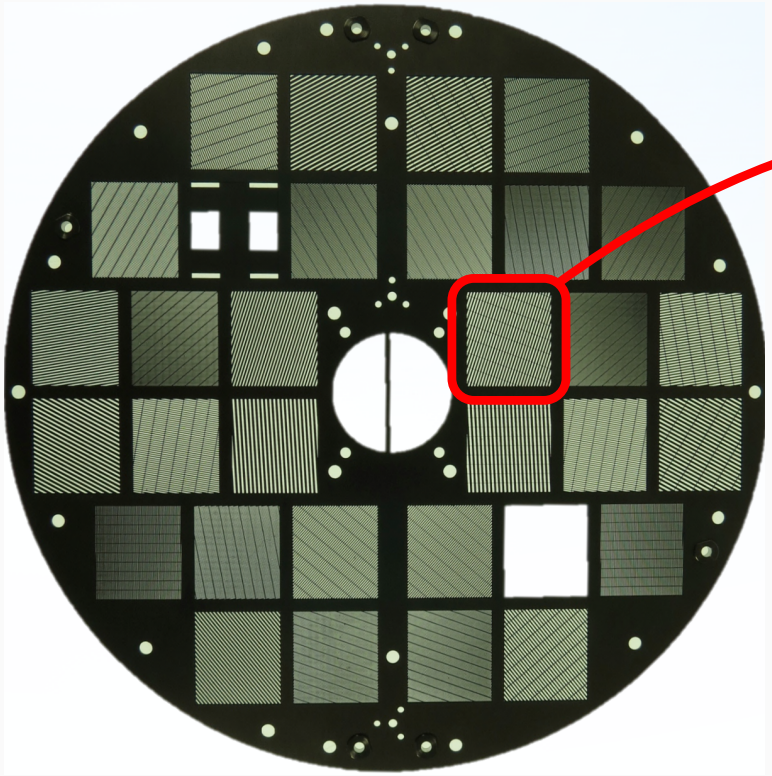

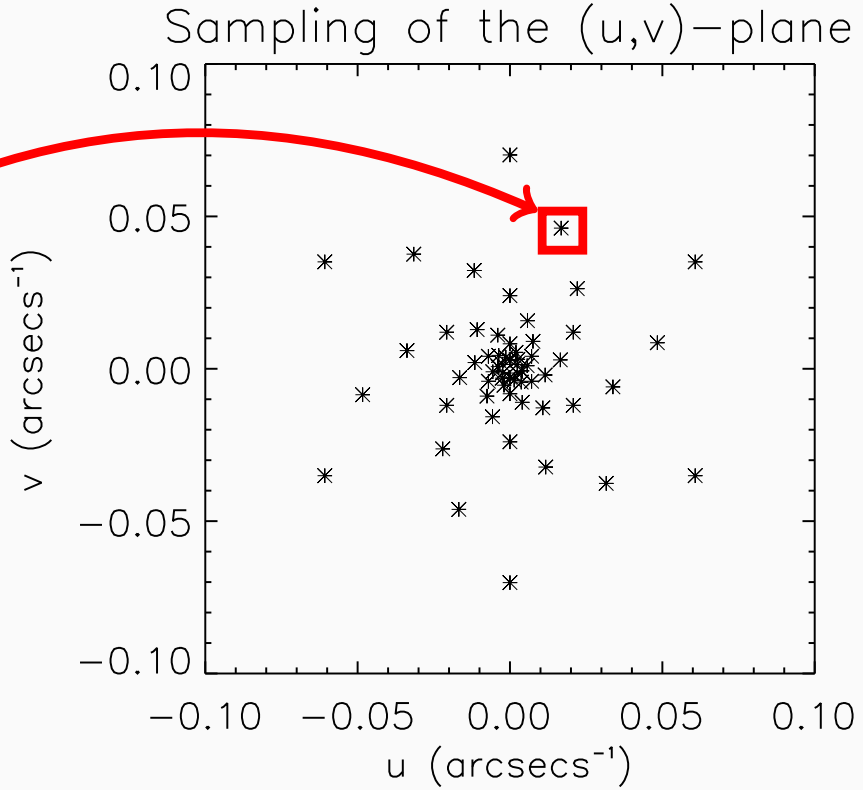

Giordano et al., 2015

$$\xi = \mathbf{k}^f \frac{L_1 + L_2}{S} - \mathbf{k}^r \frac{L_2}{S}$$

with $\mathbf{k}^{f/r} = \left(\frac{\cos \alpha^{f/r}}{p^{f/r}}, \frac{\sin \alpha^{f/r}}{p^{f/r}} \right)$.

Fourier imaging

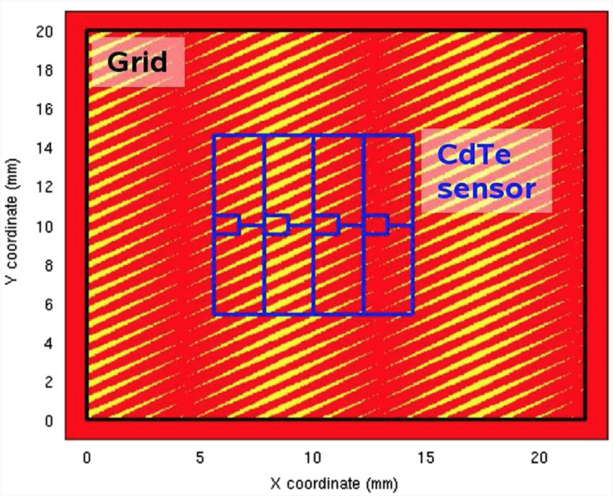

Krucker, S., Benz, A.O., et al. 2013

Fourier imaging

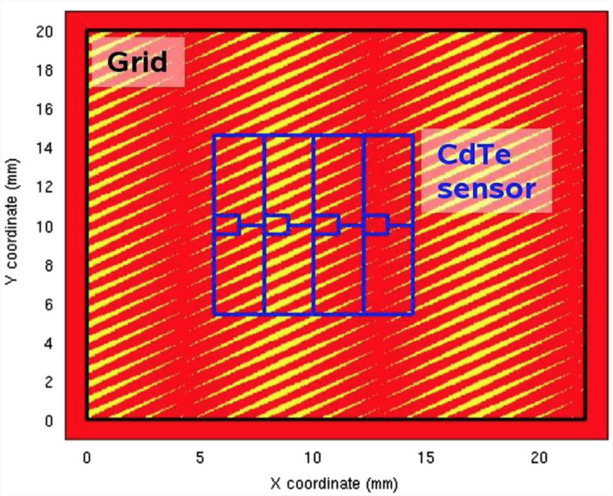

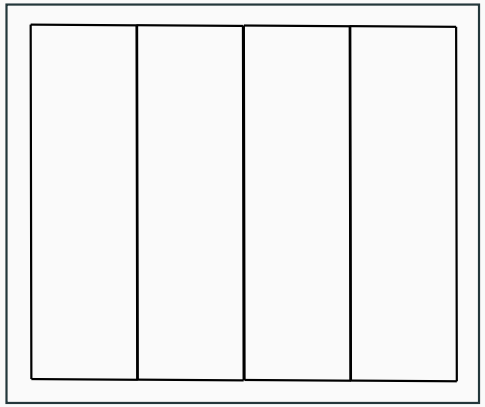

Krucker, S., Benz, A.O., et al. 2013

Fourier imaging

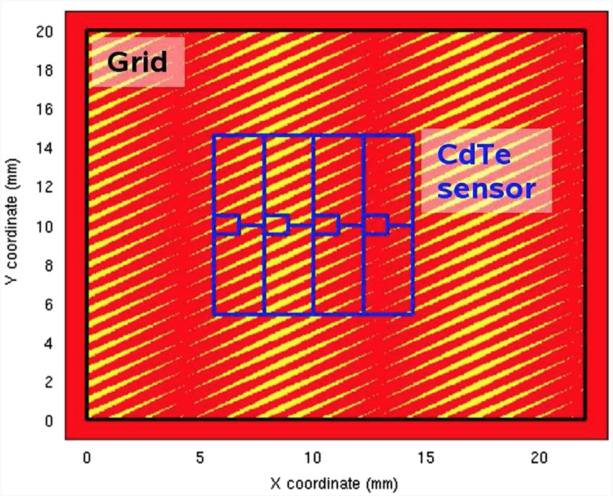

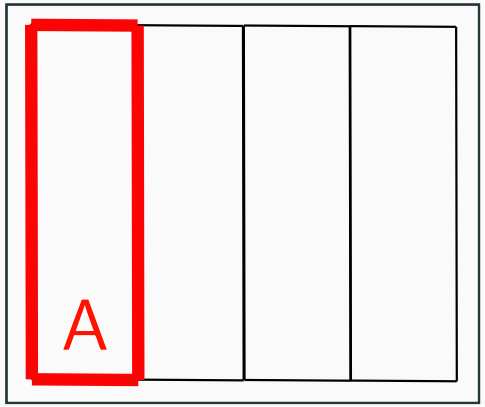

Krucker, S., Benz, A.O., et al. 2013

Fourier imaging

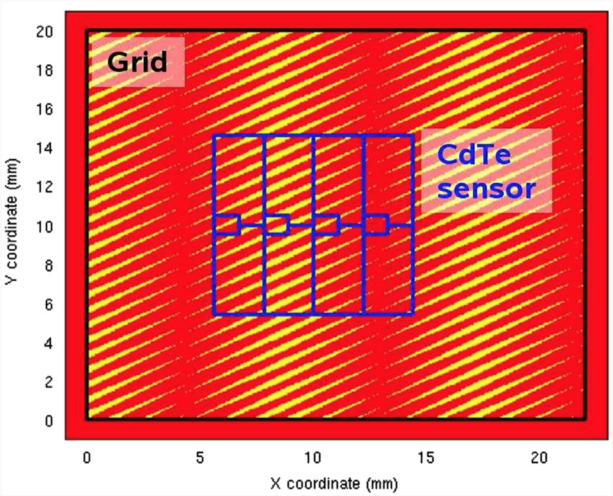

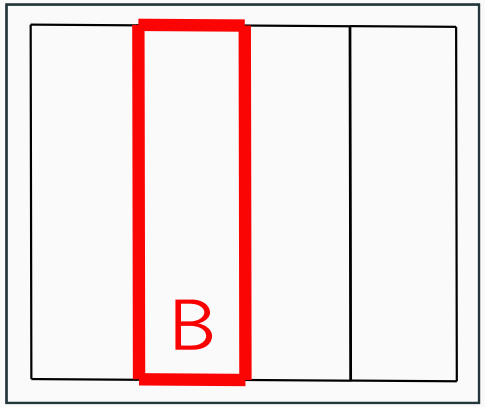

Krucker, S., Benz, A.O., et al. 2013

Fourier imaging

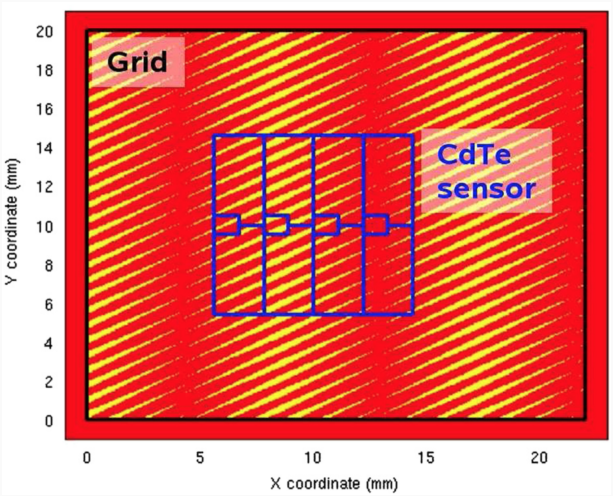

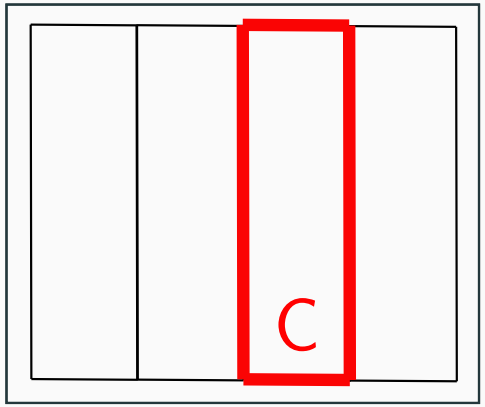

Krucker, S., Benz, A.O., et al. 2013

Fourier imaging

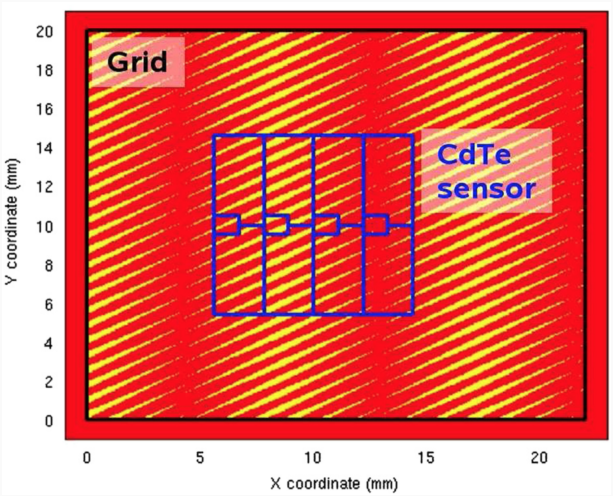

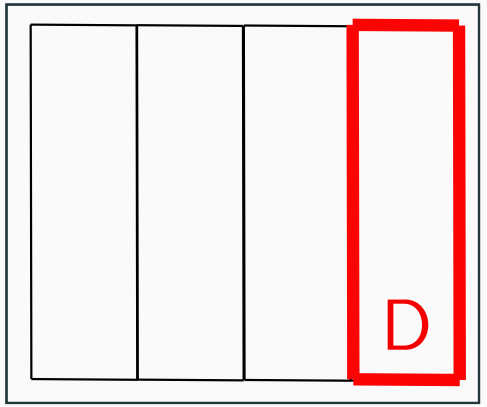

Krucker, S., Benz, A.O., et al. 2013

Fourier imaging

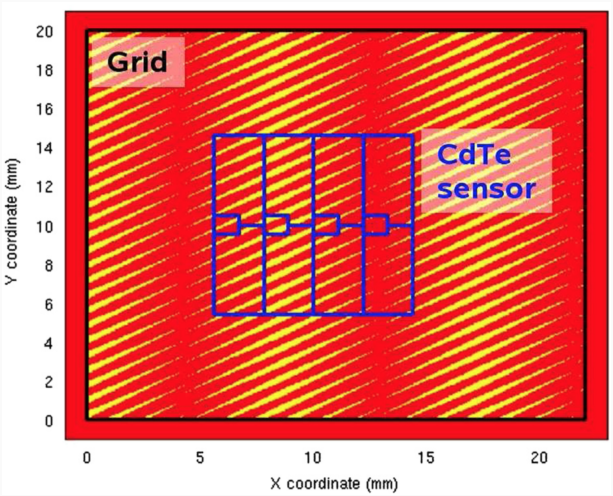

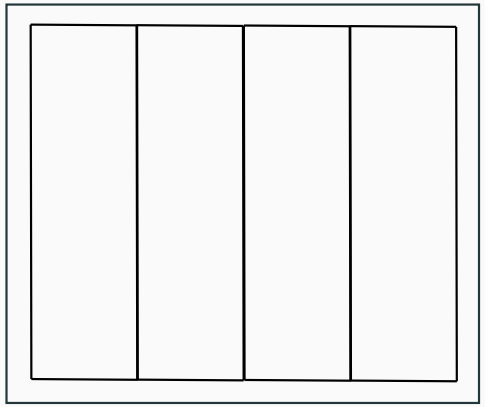

Krucker, S., Benz, A.O., et al. 2013

Visibilities formation model (Giordano et al., 2015)

The value of the visibility computed in the spatial frequency ξ sampled by the subcollimator is given by

$$V(\xi) \simeq \frac{1}{4M_1}[(\boldsymbol{C} - \boldsymbol{A}) + i(\boldsymbol{D} - \boldsymbol{B})] \exp\left(i\frac{\pi}{4}\right) \ ,$$

where M_1 is determined by hardware parameters of the instrument.

Visibility-based imaging

Image reconstruction problem from visibilities

Given $v = (V(\boldsymbol{\xi}_1), \ldots, V(\boldsymbol{\xi}_{30}))$ the vector of the visibilities measured by STIX, we want to determine the photon flux ϕ that satisfies

$$\mathcal{F}\phi = v \ ,$$

where $\mathcal{F}$ is the Fourier transform computed in the spatial frequencies $\boldsymbol{\xi}_1, \ldots, \boldsymbol{\xi}_{30}$ sampled by STIX.

Count-based imaging

Goal

We want to reconstruct the photon flux directly from count measurements, without using the visibilities.

Goal

We want to reconstruct the photon flux directly from count measurements, without using the visibilities.

- A
- B
- C
- D

Goal

We want to reconstruct the photon flux directly from count measurements, without using the visibilities.

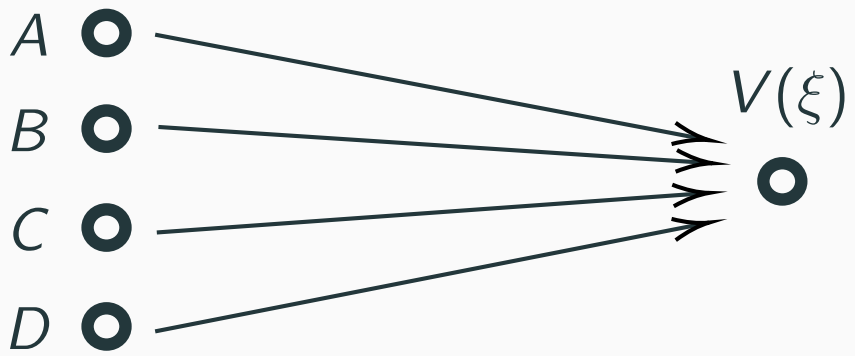

Goal

We want to reconstruct the photon flux directly from count measurements, without using the visibilities.

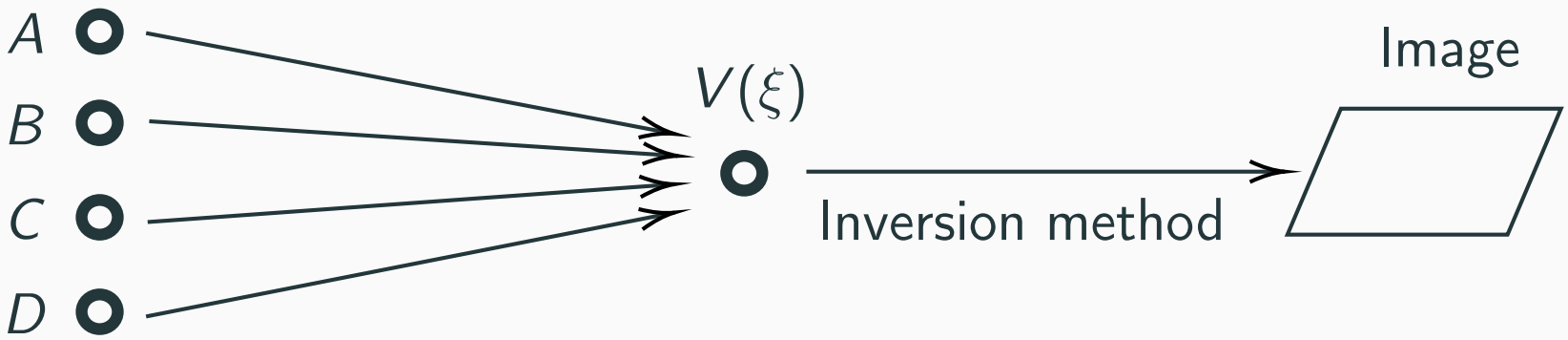

Goal

We want to reconstruct the photon flux directly from count measurements, without using the visibilities.

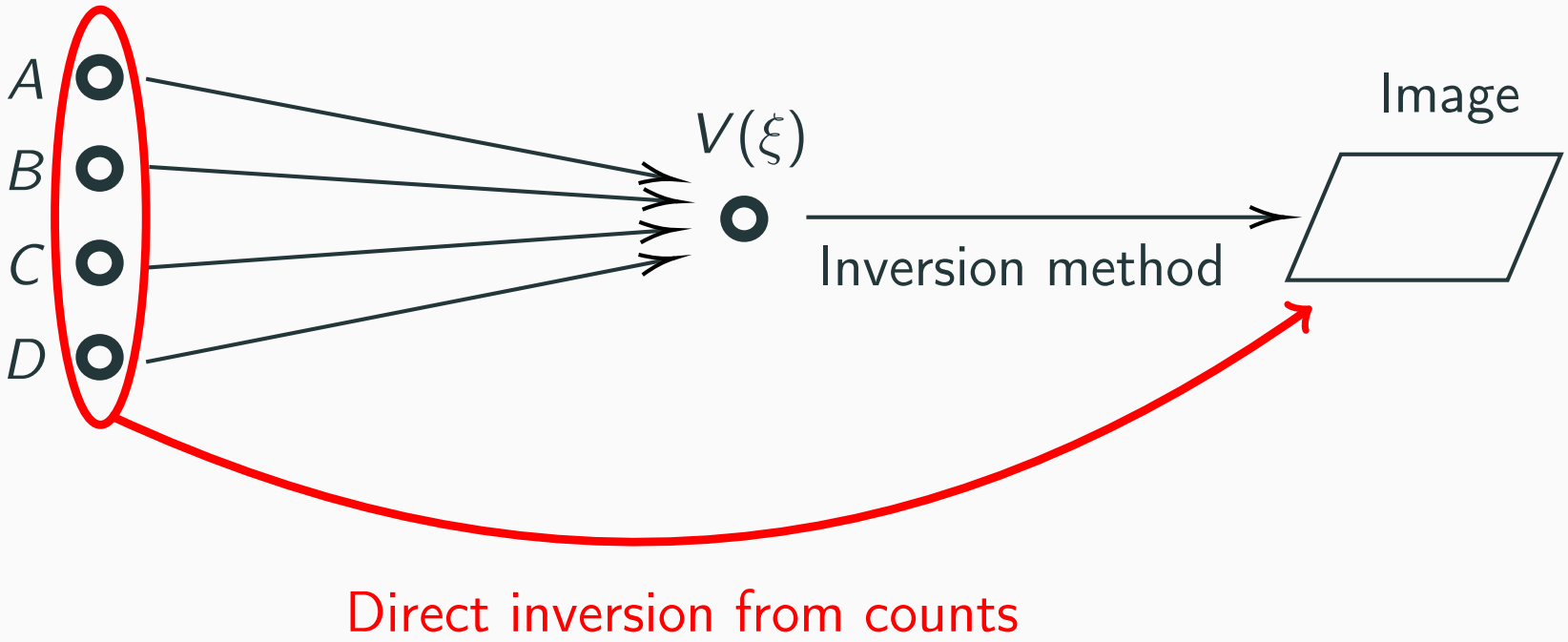

Count-based imaging

Count formation model (Massa P. et al., 2019)

The number of photon counts recorded by the pixels of a detector is given by:

$$\boldsymbol{A} \simeq \int_{\mathbb{R}^2} \phi(\boldsymbol{x}) \left(M_0 - 2M_1 \cos\left(\left(2\pi \boldsymbol{\xi} \cdot \boldsymbol{x} - \frac{\pi}{4} \right) \right) \right) \, d\boldsymbol{x}$$

$$\boldsymbol{B} \simeq \int_{\mathbb{R}^2} \phi(\boldsymbol{x}) \left(M_0 - 2M_1 \sin\left(\left(2\pi \boldsymbol{\xi} \cdot \boldsymbol{x} - \frac{\pi}{4} \right) \right) \right) \, d\boldsymbol{x}$$

$$\boldsymbol{C} \simeq \int_{\mathbb{R}^2} \phi(\boldsymbol{x}) \left(M_0 + 2M_1 \cos\left(\left(2\pi \boldsymbol{\xi} \cdot \boldsymbol{x} - \frac{\pi}{4} \right) \right) \right) \, d\boldsymbol{x}$$

$$\boldsymbol{D} \simeq \int_{\mathbb{R}^2} \phi(\boldsymbol{x}) \left(M_0 + 2M_1 \sin\left(\left(2\pi \boldsymbol{\xi} \cdot \boldsymbol{x} - \frac{\pi}{4} \right) \right) \right) \, d\boldsymbol{x}.$$

where M_0, M_1 are determined by hardware parameters of the instrument.

Count-based imaging

Counts forward operator

$$H\colon \phi \longmapsto \begin{cases} \int_{\mathbb{R}^2} \phi(\boldsymbol{x}) \left(M_0 - 2M_1 \cos\left(\left(2\pi\boldsymbol{\xi}_1 \cdot \boldsymbol{x} - \frac{\pi}{4}\right)\right)\right) d\boldsymbol{x} \\ \int_{\mathbb{R}^2} \phi(\boldsymbol{x}) \left(M_0 - 2M_1 \sin\left(\left(2\pi\boldsymbol{\xi}_1 \cdot \boldsymbol{x} - \frac{\pi}{4}\right)\right)\right) d\boldsymbol{x} \\ \int_{\mathbb{R}^2} \phi(\boldsymbol{x}) \left(M_0 + 2M_1 \cos\left(\left(2\pi\boldsymbol{\xi}_1 \cdot \boldsymbol{x} - \frac{\pi}{4}\right)\right)\right) d\boldsymbol{x} \\ \int_{\mathbb{R}^2} \phi(\boldsymbol{x}) \left(M_0 + 2M_1 \sin\left(\left(2\pi\boldsymbol{\xi}_1 \cdot \boldsymbol{x} - \frac{\pi}{4}\right)\right)\right) d\boldsymbol{x} \\ \vdots \end{cases}$$

Count-based imaging

Counts forward operator

$$H\colon \phi \longmapsto \begin{cases} \int_{\mathbb{R}^2} \phi(\boldsymbol{x}) \left(M_0 - 2M_1 \cos\left(\left(2\pi\boldsymbol{\xi}_1 \cdot \boldsymbol{x} - \frac{\pi}{4}\right)\right)\right) d\boldsymbol{x} \\ \int_{\mathbb{R}^2} \phi(\boldsymbol{x}) \left(M_0 - 2M_1 \sin\left(\left(2\pi\boldsymbol{\xi}_1 \cdot \boldsymbol{x} - \frac{\pi}{4}\right)\right)\right) d\boldsymbol{x} \\ \int_{\mathbb{R}^2} \phi(\boldsymbol{x}) \left(M_0 + 2M_1 \cos\left(\left(2\pi\boldsymbol{\xi}_1 \cdot \boldsymbol{x} - \frac{\pi}{4}\right)\right)\right) d\boldsymbol{x} \\ \int_{\mathbb{R}^2} \phi(\boldsymbol{x}) \left(M_0 + 2M_1 \sin\left(\left(2\pi\boldsymbol{\xi}_1 \cdot \boldsymbol{x} - \frac{\pi}{4}\right)\right)\right) d\boldsymbol{x} \\ \vdots \end{cases}$$

Inverse problem from counts

Given $c = (A_1, B_1, C_1, D_1, \dots)$ the vector of counts measured by STIX pixels, we want to determine ϕ such that

$$H\phi = c \ .$$

Visibilities vs counts

Advantages of the visibilty-based framework:

- algorithms can exploit FFT;
- visibilities are independent of a constant background.

Visibilities vs counts

Advantages of the visibilty-based framework:

- algorithms can exploit FFT;
- visibilities are independent of a constant background.

Advantages of the count-based framework:

- data are more noumerous;
- counts have a higher SNR with respect to the one of the real and imaginary parts of the visibilities (Massa P., et al, 2019).

RHESSI legacy

STIX will inherit a lot of image reconstruction algorithms developed for RHESSI:

Visibility-based

- MEM NJIT
- MEM GE
- VIS FWDFIT
- UV SMOOTH
- VIS CS
- VIS WV

Count-based

- Back Projection
- Clean
- Forward Fit
- Pixon
- EM

Results

Simulations

Data are simulated with a Monte Carlo method implemented in the STIX software.

Simulations

Data are simulated with a Monte Carlo method implemented in the STIX software.

Algorithms used

Visibility-based:

- VIS CLEAN (deconvolution)
- MEM GE (maximum entropy method)

Count-based:

- Expectation Maximization for Poisson data (EM)

Footpoint flare - 1

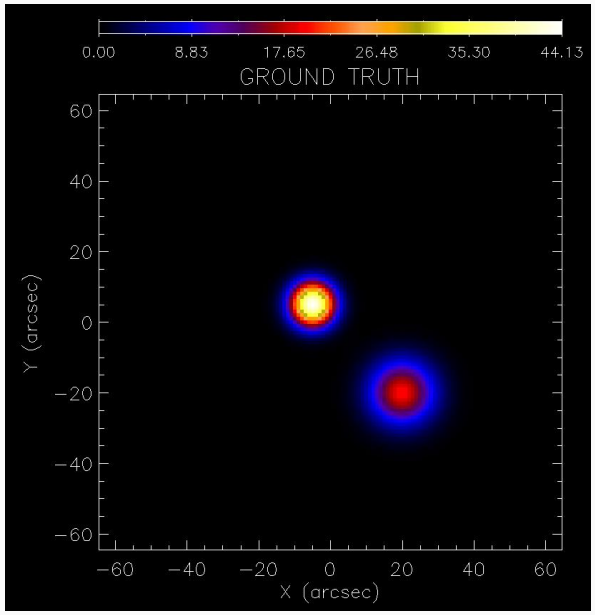

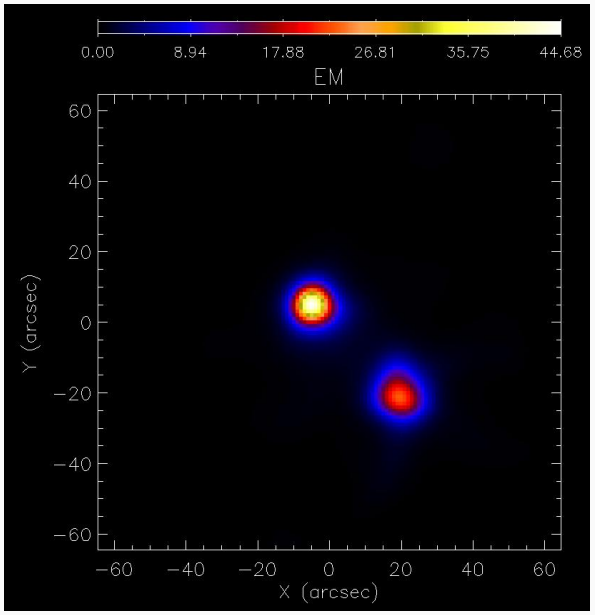

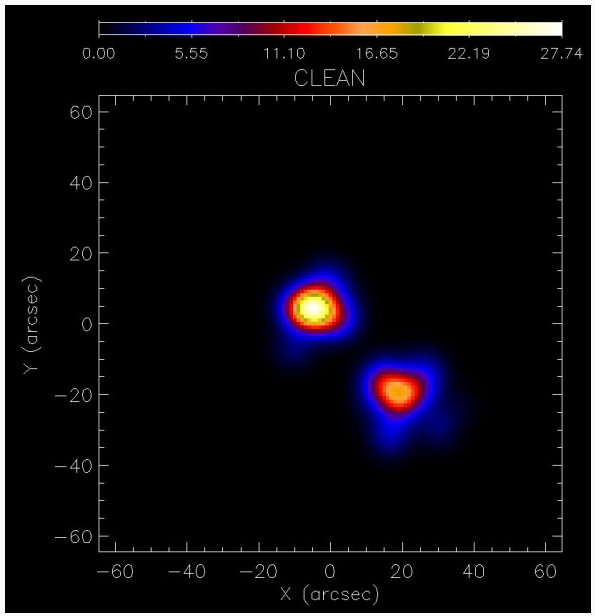

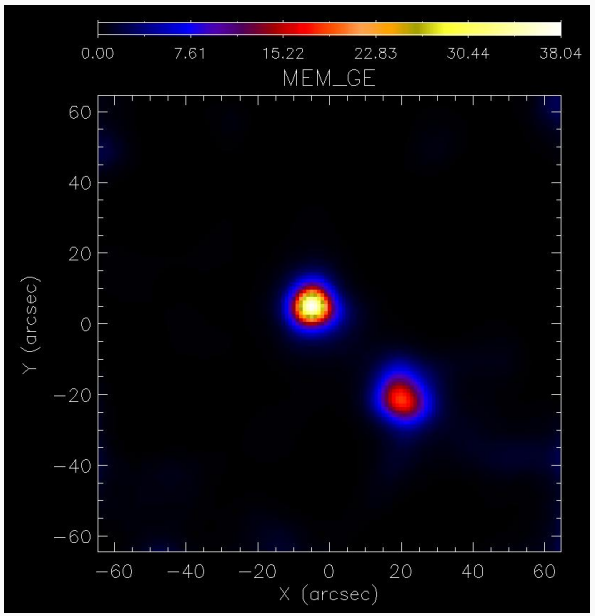

Footpoint flare - 2

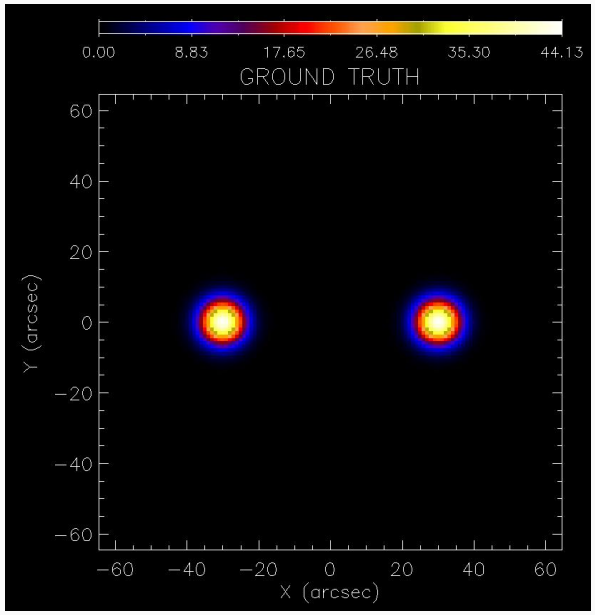

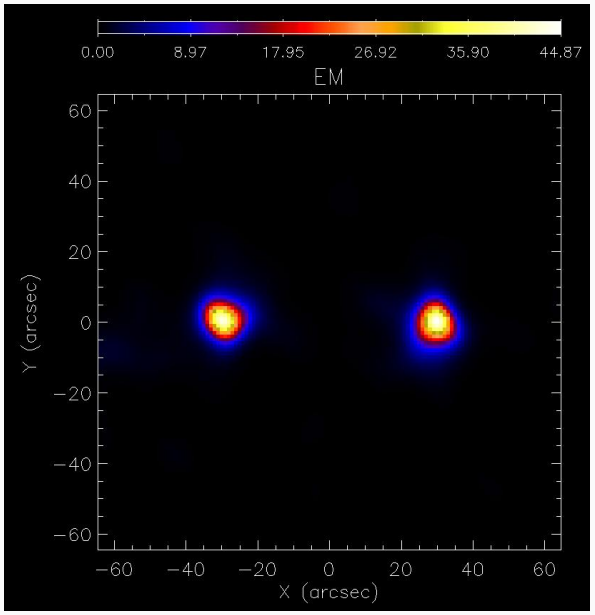

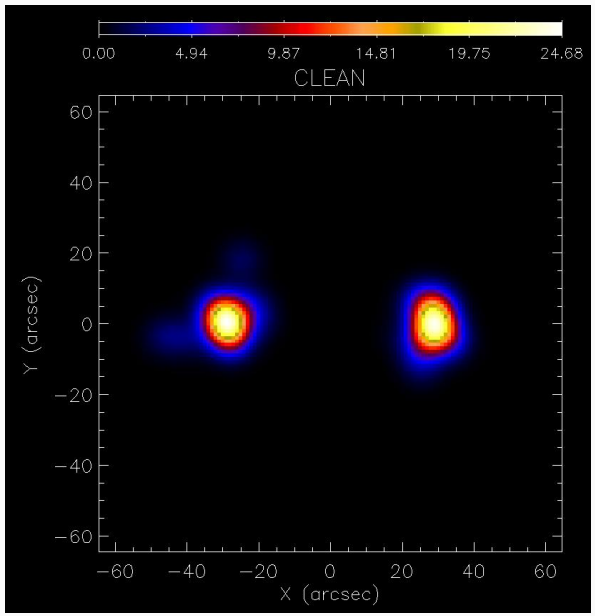

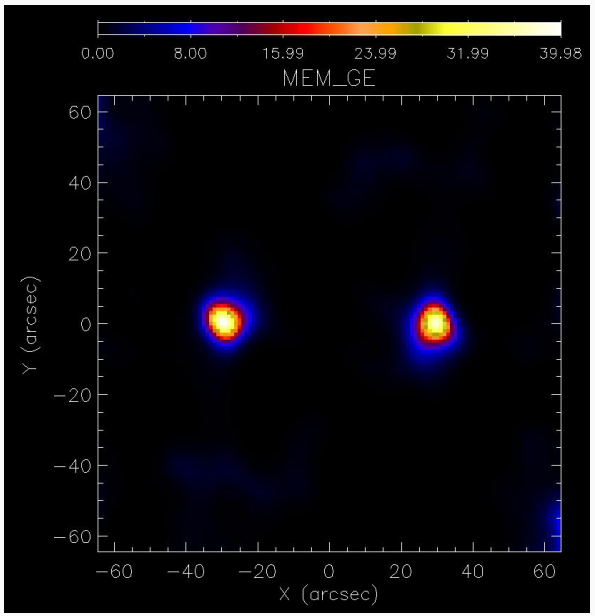

Loop flare - 1

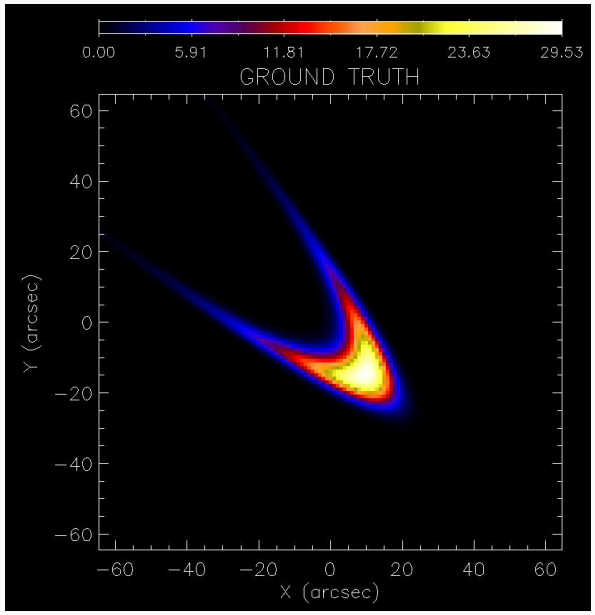
0.00 5.91 11.81 17.72 23.63 29.53
GROUND TRUTH
Y (arcsec)
X (arcsec)

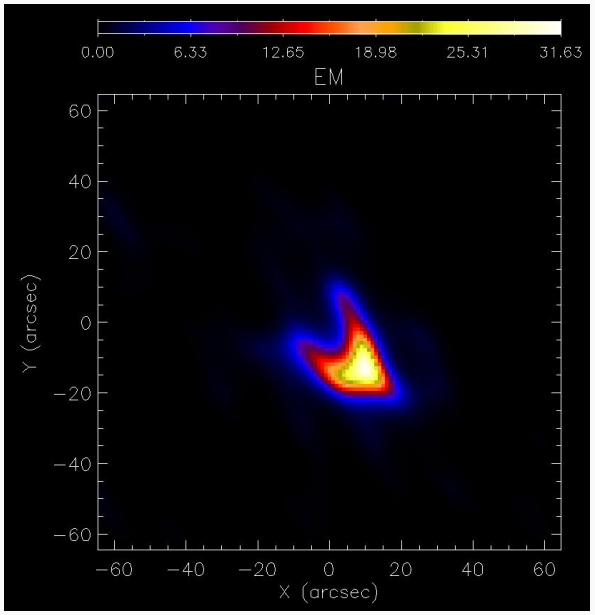
0.00 6.33 12.65 18.98 25.31 31.63
EM
Y (arcsec)
X (arcsec)

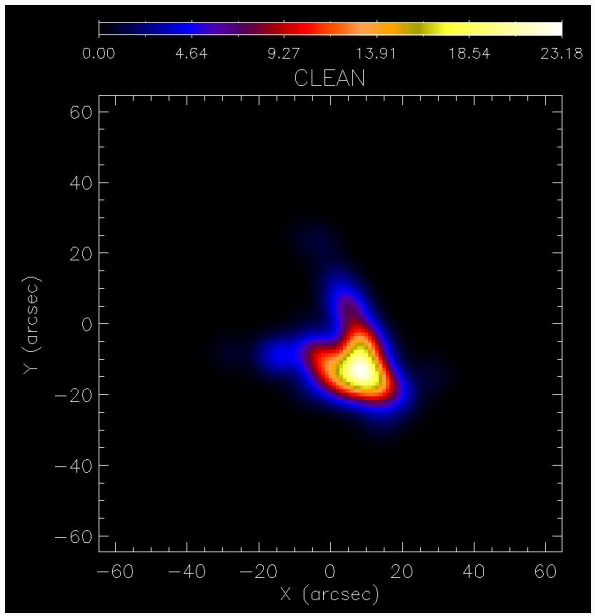
0.00 4.64 9.27 13.91 18.54 23.18
CLEAN
Y (arcsec)
X (arcsec)

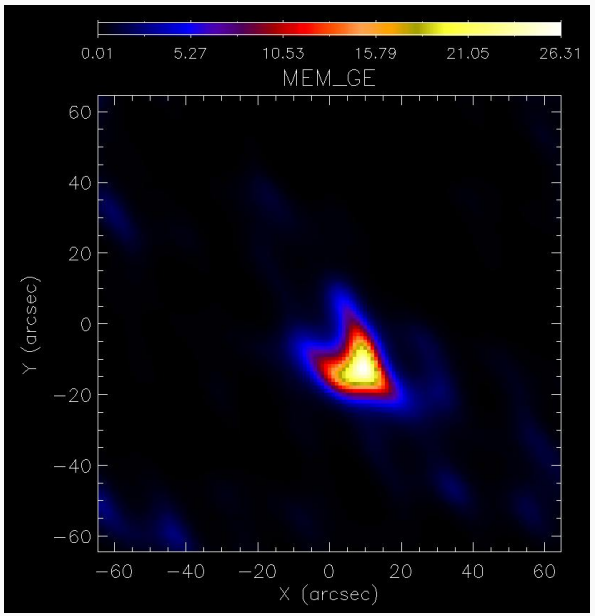
0.01 5.27 10.53 15.79 21.05 26.31
MEM_GE
Y (arcsec)
X (arcsec)

Loop flare - 2

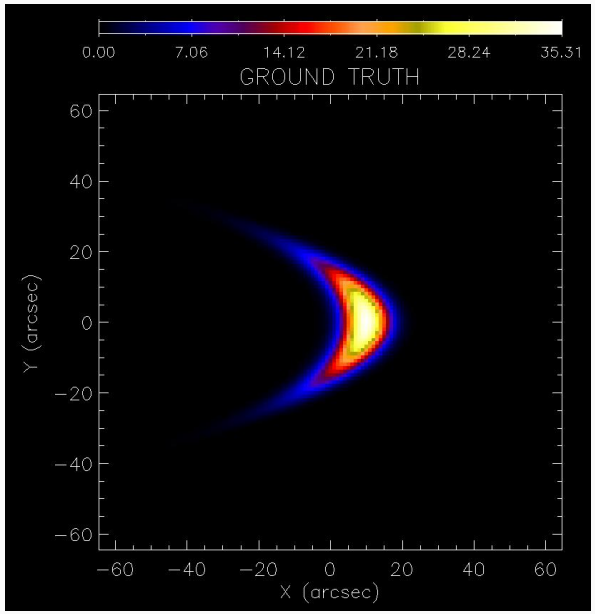
0.00 7.06 14.12 21.18 28.24 35.31
GROUND TRUTH
Y (arcsec)
X (arcsec)

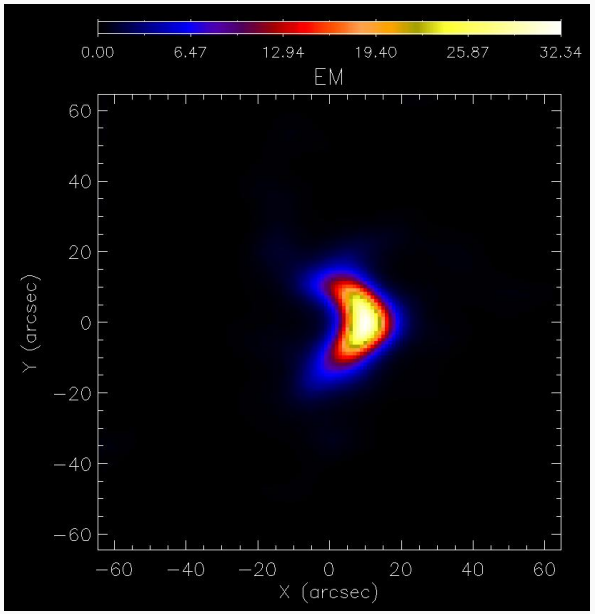
0.00 6.47 12.94 19.40 25.87 32.34
EM
Y (arcsec)
X (arcsec)

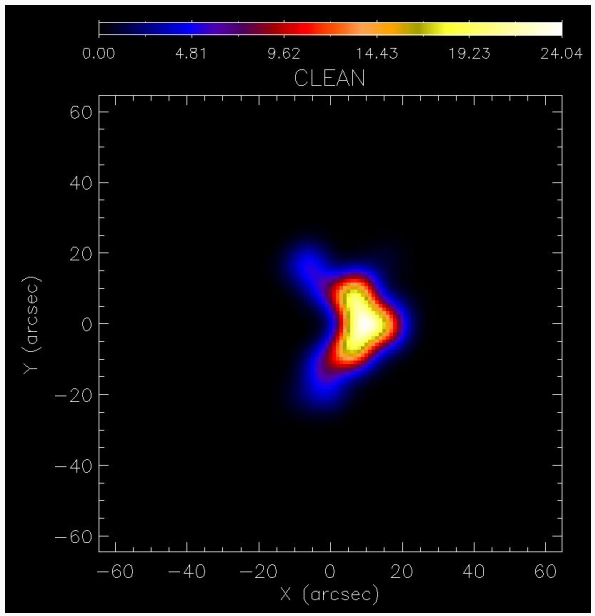
0.00 4.81 9.62 14.43 19.23 24.04
CLEAN
Y (arcsec)
X (arcsec)

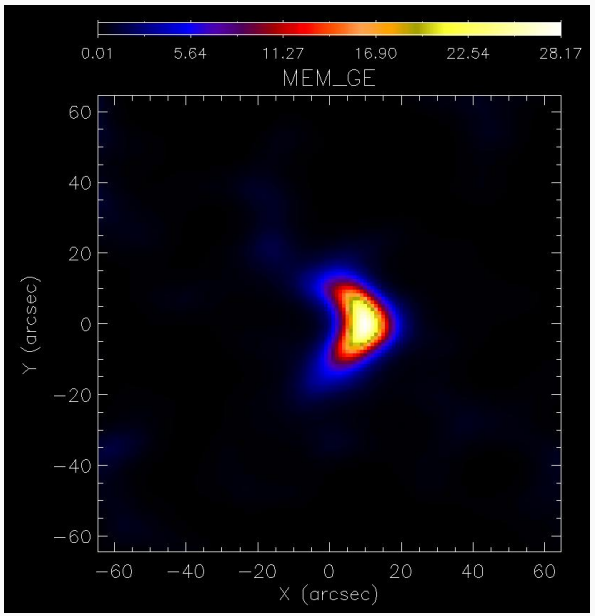
0.01 5.64 11.27 16.90 22.54 28.17
MEM_GE
Y (arcsec)
X (arcsec)

Conclusions and future work

Summary:

- we showed that STIX is a Fourier imager;
- we described the count formation model for STIX.

Conclusions and future work

Summary:

- we showed that STIX is a Fourier imager;
- we described the count formation model for STIX.

Future work:

- we will implement new algorithms for solving the STIX image reconstruction problem;
- we will refine the count formation model.

References

- Benz, A., et al. *The Spectrometer Telescope for Imaging X-rays on board the Solar Orbiter mission.* Proc. SPIE, 8443 (2012).
- Krucker, S., et al. *The Spectrometer/telescope for Imaging X-rays on Board the ESA Solar Orbiter Spacecraft.* Nuclear Inst. and Methods in Physics Research, A 732 (2013).
- Vilmer, N., Krucker, S. et al. *The spectrometer telescope for imaging X-rays (STIX) on board Solar Orbiter.* 40th COSPAR Scientific Assembly, 40 (2014)
- Giordano, S., et al. *The Process of Data Formation for the Spectrometer/Telescope for Imaging X-rays (STIX) in Solar Orbiter.* SIAM Journal on Imaging Sciences, 8.2 (2015).
- Massa, P., et al. *Count-based Imaging Model for the Spectrometer/Telescope for Imaging X-rays (STIX) in Solar Orbiter.* Astronomy & Astrophysics, 624 (2019).

References

- Benz, A., et al. *The Spectrometer Telescope for Imaging X-rays on board the Solar Orbiter mission.* Proc. SPIE, 8443 (2012).
- Krucker, S., et al. *The Spectrometer/telescope for Imaging X-rays on Board the ESA Solar Orbiter Spacecraft.* Nuclear Inst. and Methods in Physics Research, A 732 (2013).
- Vilmer, N., Krucker, S. et al. *The spectrometer telescope for imaging X-rays (STIX) on board Solar Orbiter.* 40th COSPAR Scientific Assembly, 40 (2014)
- Giordano, S., et al. *The Process of Data Formation for the Spectrometer/Telescope for Imaging X-rays (STIX) in Solar Orbiter.* SIAM Journal on Imaging Sciences, 8.2 (2015).
- Massa, P., et al. *Count-based Imaging Model for the Spectrometer/Telescope for Imaging X-rays (STIX) in Solar Orbiter.* Astronomy & Astrophysics, 624 (2019).

Thank you for the attention!